JET-P(95)70

Unanswered Questions in Ion-Temperature-Gradient-Driven Turbulence

M Ottaviani, M A Beer[1], S Cowley[2], W Horton[3], J Krommes[1].

JET Joint Undertaking, Abingdon, Oxfordshire, OX14 3EA, UK.
[1] Plasma Physics Lab., Princeton University, PO Box 451, Princeton, NJ 08543.
[2] Dept. of Physics, UCLA, 405 Hilgard Ave., Los Angeles, CA 90024-1547.
[3] IFS, University of Texas at Austin, Austin, TX 78712-1060.

Preprint of a paper to be submitted for publication in the
Proceedings of the ITP Program on
Intermittent and Turbulent Phenomena in Plasmas

November 1995

Contents

Abstract

In this work a number of open questions in the theory of ion-temperature-gradient-driven turbulence are considered. A simple model is introduced as a paradigm of more complex plasma turbulence models. Special emphasis is placed on those issues that are relevant for the understanding of turbulent transport.

1 Introduction

Understanding plasma turbulence is perhaps the greatest challenge facing theoretical research in the field of plasma physics.

Turbulent plasma motion occurs in a variety of laboratory as well as natural plasmas. Not unexpectedly, this widespread phenomenon occurs in a variety of types. This is quite natural, as plasmas are highly complex fluids. Indeed, from the fluid dynamics point of view, plasmas are multicomponent fluids characterized by a variety of space and time scales; they can be constrained by complicated geometries and are subject to anisotropies and inhomogeneities.

A substantial fraction of the theoretical effort has been oriented towards understanding plasma turbulence in magnetic confinement devices. This is due to the fact that some form of plasma turbulence is commonly thought to be the underlying cause of particle and heat transport in these devices. Heat losses are a severe limiting factor towards reaching high temperature plasmas at an acceptable energy cost, and thus achieving ignition: the condition of self-sustained burning plasmas that is a primary goal of fusion research.

Among the various confinement machines that have been built, tokamaks are the most successful so far. Tokamaks are toroidal confinement devices designed to operate with magnetic field configurations possessing rotational symmetry around the machine axis. It is an experimental fact that tokamaks normally operate under conditions of small deviations from axisymmetry. When magnetic activity is recorded it is usually identified as the formation of a small, isolated magnetic island chain. Although such a structure breaks the axisymmetry, the incremental transport it causes is small and cannot account for the observed particle and heat losses.

One should remark that much debate has been devoted to whether there exist smaller (but numerous) island chains which escape detection because of their size but whose effect on transport is not negligible. Presently this hypothesis does not seem to receive much favor. Indeed, on the theoretical side, it is difficult to justify the formation of islands of sufficiently high amplitude to cause the observed transport. On the experimental side, the nature of the observed transport seems to differ from what one would expect from the existence of such islands. Experimental measurements on TFTR indicate that in the absence of macroscopic MHD instabilities, these magnetic islands are not present, or are too small to be detected [1].

Therefore most of the theoretical effort to understand tokamak transport has been oriented towards electrostatic turbulence. Electrostatic turbulence refers to a type of turbulence that is assumed to satisfy the electrostatic approximation. Although virtually any conceivable plasma motion would cause a perturbed current and hence a perturbed magnetic field, there is a large class of plasma dynamics models where a perturbation of the vector potential does not enter in the model equations to the leading order in the relevant expansion parameter. This is the electrostatic approximation: only the fluctuating electrostatic potential survives. The fluctuating magnetic field can be computed afterwards but its effect on transport turns out to be negligibly small. The main source of transport in electrostatic turbulence is the $\mathbf{E} \times \mathbf{B}$ motion of the charged particles in the fluctuating electric field.

As one may have expected from such a complex fluid, the electrostatic approximation is not the only simplification one has to introduce in order to obtain a workable model of the plasma dynamics. Even considering pure plasmas and ignoring wave-particle resonances, the model one can conceivably build would require at least five scalar fields defined on a three-dimensional spatial domain as dependent variables. Such a model would depend on a large number of control parameters. One can easily see that a detailed analytical treatment of such a model would be impractical.

Thus one is lead to further simplifications. Often the reduction process is guided by the analysis of the linearized equations. One considers the problem of the stability of the axisymmetric configuration towards various symmetry-breaking perturbations. Once an instability is found, one proceeds by identifying the "drive" of the instability, usually the gradient of some equilibrium quantity. The reduction process involves keeping in the model only those fields which are essential to the linear description of the instability. The ensuing turbulent state which occurs when the instability is saturated is termed after the instability drive.

One should point out that there is an obvious drawback with this way of classifying the types of plasma turbulence. Indeed one quickly realizes that different kinds of instabilities can lead to qualitatively similar turbulent behavior. Many details of linear theory, which take a part, for example, in determining the instability threshold, are not relevant for the turbulent dynamics.

Moreover, on the basis of general experience with nonlinear dynamics, one expects that some selection processes are at work during the nonlinear evolution of an instability. For example, two nonlinearities which would appear of nominally comparable importance with respect to the orderings of linear theory could play roles of substantially different importance in the nonlinear evolution. If this turns out to be the case, concepts hinging on the idea of universality could play a role in limiting the types of qualitatively distinct turbulent motions to a handful.

From this preliminary discussion one can appreciate the complexity of the plasma turbulence problem. Thus one can expect that progress would initially come from the analysis of "paradigm models" —i.e., models designed to retain some elements of the actual plasma dynamics without "unwanted" complications.

As such, paradigm models are rather subjective. The best known examples, the

Hasegawa–Mima [2] and the Terry–Horton [3] models, have been very useful in understanding a number of basic features of homogeneous plasma turbulence. However these models are too simple to be used as paradigms to investigate plasma transport of the type considered relevant for tokamaks.

Thus, in the past few years the main body of investigation has been focused on a certain class of plasma dynamics models in which the ion temperature gradient (ITG) plays a central role. In the ITG model, nonadiabatic electron dynamics is neglected, isolating the ion temperature gradient as the sole drive for the ensuing turbulence. While this model cannot address issues of particle transport or turbulence driven by trapped electron modes, ion heat transport can be calculated accurately, since nonadiabatic electron dynamics has little impact on the ITG instability in many physically relevant parameter regimes. It is thus natural to consider plasma dynamics paradigms belonging to the ITG class.

1.1 ITG turbulence

Generically, one can define the ion-temperature-gradient-driven (ITG) turbulence as a type of plasma turbulence produced and sustained by ion temperature gradients.

When looking at the linear theory of ITG, one meets a large body of detailed analysis in various situations of practical interest. In order to have an instability, the ion temperature gradient must be combined with the effect of something else. Commonly one considers the magnetic curvature and/or the parallel compressibility, but the addition of an impurity species and other effects have also been studied.

In this work, however, taking the previously outlined viewpoint, no attempt will be made to classify the various subtypes of ITG. Rather, a relatively simple model (a minimal model) of ITG turbulence will be introduced, quite liberally ignoring a number of terms one would obtain from the formal derivation. The goal is to obtain something workable which can be used to identify the main theoretical questions awaiting an answer.

1.2 Outline of this work

The plan of this work is as follows. Sec. 2 is devoted to the simplest ITG equations which retain the essential features. In Sec. 2.1 the model equations are presented. Sec. 2.2 presents a brief review of the main results of linear theory, and Sec. 2.3 summarizes the results of numerical investigations.

The subsequent sections are devoted to the open problems. Sec. 3 deals with the problem of the dependence of the correlation length and time of ITG turbulence. First, the evaluation of the correlation length of homogeneous turbulence is outlined. Then, the mixing length concept in fluid dynamics is reviewed (Sec. 3.2), and the questions arising when one tries to apply it to ITG are presented.

Sec. 4 discusses the possible role of coherent structures.

Sec. 5 is devoted to nonlocal effects. The possible influence of the boundary layers is discussed in Sec. 5.1, and Sec. 5.2 discusses nondiffusive effects.

Conclusions are drawn in Sec. 6.

2 The model

This section is devoted to the presentation of simple model equations, to a summary of the results of linear theory, and to a brief review of the progress in understanding ITG turbulence that has derived from numerical simulations.

2.1 Basic ITG model equations

We consider a toroidally confined plasma possessing a simple (low β) axisymmetric equilibrium with circular magnetic flux surfaces. This magnetic equilibrium is fully characterized by the safety factor $q(r)$, the minor and major radii a and R, and the toroidal magnetic field B on axis. Since we consider electrostatic turbulence, we assume that the magnetic field does not change with time. Thus from the point of view of the charged particles, the main effect is the $\mathbf{E} \times \mathbf{B}$ motion across the field lines and the free-streaming motion along the field lines.

Thus a minimal model of ITG dynamics must describe the evolution of three fields: the electric potential ϕ which causes motion perpendicular to the field lines, the parallel ion velocity v which describes the plasma motion along the field lines, and the ion temperature T whose gradient is the turbulence source.

A formal derivation of a general ITG model could be obtained from a low-frequency expansion starting from the general fluid equations of plasma dynamics [4] or preferably from a closure of the moment hierarchy of the gyrokinetic equation [5, 6, 7, 8, 9, 10].

The model presented below can be derived from the 3+1 (three parallel velocity moments and one perpendicular velocity moment) fluid equations of Ref. [10] by imposing pressure isotropy, assuming constant equilibrium density, and omitting certain damping terms that are not essential for the present discussion.

In summary, one obtains the set of equations:

$$dn/dt + 2\epsilon\partial_Z(\phi + T) + A\nabla_{\|}v = 0, \tag{1}$$

$$dv/dt + A\nabla_{\|}(\phi + T) = 0, \tag{2}$$

$$dT/dt + \Gamma A\nabla_{\|}v = -A|\nabla_{\|}|T, \tag{3}$$

where $n = \phi - \langle\phi\rangle - \rho_*^2\nabla^2\phi$ is the density. The operators are the advection operator $d/dt = \partial_t + \mathbf{v}_E \cdot \nabla$, the curvature operator $\partial_Z = (\cos\theta/r)\partial_\theta + \sin\theta\partial_r$ and the parallel gradient operator $\nabla_{\|} = (1/q)(q\partial_\phi + \partial_\theta)$. The operator $|\nabla_{\|}|$ symbolically represents the nonlocal operator which is $|k_{\|}|$ in Fourier space, and models parallel Landau damping [5]. $\langle\bullet\rangle$ is the flux-surface-averaging operator. The explicit control parameters are $\rho_* = \rho_s/a$ (ρ_s is the ion Larmor radius evaluated at the electron temperature) and $\epsilon = a/R$. Other control parameters are needed to parametrize the profiles (those that are held fixed) and the boundary conditions when appropriate (e.g., the incoming heat flux). A is defined as ϵ/ρ_* and Γ is just a numerical constant of order unity.

We have chosen to employ "large scale" units by normalizing the lengths to a, the time to a^2/D_B ($D_B = cT_e/eB$ is the Bohm diffusivity), and the fields to T_e/ϵ, c_s

and T_e. This seems the natural choice when no a priori assumption is made about the scaling of the various quantities with the scale separation parameter ρ_*. When, however, an expansion is made in ρ_*, the macroscopic scales a and R drop out of the problem, as discussed in Sec. 2.3, below.

The term in the RHS of Eq. 3 describes Landau damping; it is essential in setting a large-scale cutoff to the unstable modes. Other damping terms could be added to model various relevant dissipation mechanisms. Note however that, in the spirit of this paper, no attempt will be made at discussing the various damping terms that one could derive from a systematic approach [10].

Eqs. 1–3 clearly exhibit the $\mathbf{E}\times\mathbf{B}$ advection in the perpendicular direction of the plasma density, energy, and parallel momentum combined with the streaming along the field lines.

2.2 Linear theory

We now briefly review the stability properties of this ITG model when the system is subject to a given constant temperature gradient. We take $\nabla T = -(T_e/L_T)\hat{r} + \nabla\tilde{T}$, where the equilibrium ion and electron temperatures have been assumed to be equal and the temperature gradient scale length L_T has been introduced. It is natural to use this length instead of a when discussing linear theory and, for this section only, we rescale the various quantities accordingly.

It is initially convenient to proceed through a naive linear theory, ignoring the spatial dependence of the equilibrium quantities and replacing the spatial derivatives with constant wavevectors $\nabla \to i\mathbf{k}_\perp$ and $\nabla_\| \to ik_\|$.

The resulting dispersion relation has the form

$$\hat{\omega}^3 + \hat{\omega}_d\hat{\omega}^2 + [\hat{\omega}_T^*\hat{\omega}_d - (1+\Gamma)]\hat{\omega} - \hat{\omega}_T^* + i(\hat{\omega}^2 + \hat{\omega}_d\hat{\omega} - 1) = 0, \qquad (4)$$

where it is convenient to normalize once more the frequencies to the sound frequency $\hat{\omega} \equiv \omega/(Ak_\|) \equiv \Omega/(c_s k_\|)$, etc. We denote with Ω the dimensional frequency and with ω the dimensionless counterpart.

Eq. 4 exhibits the two classic ITG roots. First, we observe that with large temperature gradients the first and the third term balance to give the interchange type branch whose growth rate behaves as:

$$\hat{\gamma} \approx (\hat{\omega}_T^* \hat{\omega}_d)^{1/2}. \tag{5}$$

When the curvature term $\hat{\omega}_d$ can be ordered small one obtains the slab-type branch with growth rate:

$$\hat{\gamma} \approx (\hat{\omega}_T^*)^{1/3}. \tag{6}$$

In both cases the imaginary part can be ordered small for sufficiently small parallel wavelength.

Absolute stability is achieved for sufficiently low ratios of the forcing (temperature gradient) to the damping (parallel wavelength). By forcing $\hat{\omega}$ to be real one obtains the marginal stability condition (one can verify that the other roots are stable):

$$\hat{\omega}_T^{*2} + \Gamma \hat{\omega}_T^* \hat{\omega}_d - \Gamma^2 = 0. \tag{7}$$

The middle term is subdominant in the situations of interest $\hat{\omega}_d \ll \hat{\omega}_T^*$. The resulting stability condition can be written in the dimensional form (omitting a constant of order one):

$$\omega_T^* \leq c_s k_{||}, \tag{8}$$

which emphasizes the stabilizing role of the ion Landau damping.

The problem with this naive approach to linear theory is the inhomogeneity. Whereas, in the spirit of the WKB approximation, the wavelength perpendicular to the field lines can be taken much shorter than the equilibrium scale length, the same does not hold in the direction parallel to the field lines. This is revealed by the above calculation, which shows that instability occurs when $k_{||}$ is in some sense small.

The well known ballooning transformation [11] is designed to deal with this situation. It is convenient to employ field line coordinates as advocated by Cowley *et al.* [12]. For the simple equilibrium under consideration this amounts to the transformation:

$$\begin{aligned} x &= r, \\ y &= q(r)\theta - \phi, \\ z &= \theta. \end{aligned} \tag{9}$$

The important point here is that the parallel derivative becomes the derivative along z: $\nabla_{\|} \to (1/q)\partial_z$. The WKB approximation can still be "partially" employed in the perpendicular coordinates: $\partial_x \to ik_x$, $\partial_y \to ik_y$. To the leading order one obtains an ordinary differential equation in z. The outcome is a local eigenvalue which depends parametrically on the other spatial variables.

Most of the linear theory of microinstabilities in toroidal geometry, including ITG [13, 14, 15], has been worked out to the leading order only. This calculation gives qualitative agreement with the previous analysis, as far as the growth rate and the instability threshold of short wavelength modes is concerned. However, a weakly unstable branch can survive even at remarkably long wavelengths [15].

Renewed interest in linear theory has been stimulated by recent works that analyze the second-order equations of the WKB ballooning approximation to determine the radial structure (envelope) of the eigenfunctions [16, 17, 18]. The remarkable outcome of these calculations is that the radial extension of the eigenfunctions δr scales typically as

$$\delta r \sim (\rho_s a)^{1/2}. \tag{10}$$

Structures resembling the linear eigenfunctions of Refs. [16, 17, 18] are reported in recent toroidal simulations [19]. These results have prompted a debate whether Eq. 10 should be used to estimate the radial correlation length of ITG turbulence. We come back to this point in Sec. 3.

2.3 Numerical investigations

Numerical work on ITG has been performed since the early investigation of Horton et al. [20]. However, only in the last few years has adequate resolution been employed with reliable models of the relevant physics, thanks to the increase in computer power and to the use of field-line coordinates [12] in flux tube simulations [21]. To date, most of the effort has been concentrated on increasing the physics content of the simulations to obtain closer quantitative agreement with experimentally measured transport levels. By comparison, less effort has been made to understand the basic questions that are the subject of this work. The significant progress made so far is briefly reviewed in this section.

For parameters typical of present day and future tokamaks, the dominant dissipation in ITG turbulence arises from collisionless Landau damping. The earliest fluid models [4] ignored this damping, so artificially large collisional damping was added to the simulations at short wavelengths to provide a sink for the fluctuation energy. Recently, two complementary approaches have included the effects of Landau damping and other wave-particle resonances: 1) gyrokinetic particle simulations which solve the gyrokinetic equation in three space dimensions and two velocity-space dimensions [22], and 2) gyrofluid simulations which solve reduced fluid equations in three space dimensions [5, 6, 7, 8, 9, 10]. These gyrofluid equations contain closure approximations to model the wave-particle resonances, leading to physics-based damping mechanisms.

Another area of development has been the use of reduced simulation volumes. The most straightforward approach is to simulate an entire tokamak (full torus simulations [23]) including sources and sinks of particles and energy. These simulations are computationally most challenging because they must simultaneously resolve a wide range of space and time scales. Fluctuation measurements in tokamaks find turbulent correlation lengths $L_c \sim 10\rho_i \sim 1 - 2\,\mathrm{cm}$ perpendicular to $\mathbf{B}$ [24], while the largest scale which must be resolved is the minor radius, $a \sim 100\,\mathrm{cm}$. Similarly, the turbulent time scales, of order $10 - 100\,\mu\mathrm{sec}$, are much shorter than the transport time scales, of order 100 msec. This scale separation motivated the gyrokinetic ordering [25], an expansion in the small parameter $\rho_i/L \sim \varepsilon$, where L is the scale length for the equilibrium variations — e.g., $L_T = T_0/|\nabla T_0|$. The fluctuation time scales and magnitudes are ordered small, $1/\tau_c\Omega_i \sim e\Phi/T \sim F_1/F_0 \sim \varepsilon$, and the turbulent length scales are of order $L_c \sim \rho_i$. Although the distribution function has been broken into fluctuating (F_1) and equilibrium (F_0) parts, the ordering retains strong nonlinearity, since $\nabla F_1 \sim \nabla F_0$. In this ordering, the transport time scale (the time scale for relaxation of the equilibrium) can be found from the energy balance equation, $\frac{3}{2} n_0 \partial T_0/\partial t \sim \nabla \cdot Q$, where $\partial T_0/\partial t \sim T_0/\tau_{eq}$. The heat flux arises from the fluctuations, so $Q \sim n_0 \chi \nabla T_0 \sim n_0(L_c^2/\tau_c)(T_0/L_T)$, where L_c and τ_c are the length and time scales of the fluctuations. Thus $\tau_{eq} \sim \tau_c/\varepsilon^2$, and on the fluctuation time scale (or the length of the simulation), the equilibrium can be held fixed. This ordering is well satisfied in the core of present-day tokamaks, but becomes less well satisfied near the plasma edge. For example, in the core of TFTR, the equilibrium scales L_n and L_T are longer than 20 cm for $r/a < 0.85$, while the measured $L_c \approx 1 - 2$ cm. The gradients steepen near the edge and L_{eq} can be as small as 1–10 cm for $r/a > 0.85$. The breakdown of the gyrokinetic expansion may permit boundary layer effects as discussed in Sec. 5.1.

This scale separation has motivated the use of flux tube simulation domains. Instead of simulating the full torus with sources and sinks, one need only simulate a thin flux tube that is several turbulent correlation lengths in each direction, leading to significant computational savings [21]. On the fluctuation scale L_c, the equilibrium variations are assumed to be weak ($L_c \ll L_{eq}$) and thus the plasma equilibrium is fully specified by the temperature and density gradients L_T and L_n. Over the time scale of the simulation (several τ_c), L_T and L_n can be considered constant in space and time. The heat flux Q across a given flux surface can be calculated as a function of these local parameters, and can then be compared with the experimental heat fluxes. Because the calculated transport is quite sensitive to small uncertainties in the equilibrium gradients, better quantitative agreement with experiments has been obtained by parameterizing the simulation results in terms of the equilibrium quantities, and then using this parameterized heat flux in self-consistent transport calculations which solve for the evolution of the equilibrium on the much longer transport time scale [26]. This approach has been used with considerable success.

These more detailed simulations have revealed several interesting features of ITG turbulence. Toroidal effects arising from the ∇B and curvature drifts have been found to dramatically increase (by a factor ~ 25) the turbulent heat flux [10] compared to similar simulations in sheared slab geometry [9], bringing the calculated heat flux up to experimentally measured levels. An important feature in the development of the turbulence is the role played by the nonlinear generation of sheared $\mathbf{E} \times \mathbf{B}$ flows, and the collisionless damping of the poloidal component of this rotation. The simulations find that the peak of the fluctuation energy at saturation is at longer wavelengths than the fastest growing instabilities, and the radial and poloidal fluctuation spectra are in qualitative agreement with those measured experimentally [24, 21]. It has been found that much of the variation in the calculated heat flux can be described by the estimate $Q \sim \max(\gamma/k_\perp^2)$ [26], although this approximation remains to be justified on purely theoretical grounds. These simulations draw attention to several interesting questions, as discussed in the remainder of this paper. Ideally, the simulations would be used as a guide in developing a theoretical parameterization of the transport in terms of the equilibrium. The recent favorable comparison of simulation and experimental results suggest that these simulations are a relevant tool to address these questions. Simultaneously, new physics is being added to the simulations to address a wider range of experimental behavior and parameter regimes.

2.4 Statistical closures

Although statistical closures (SC's) represent a well developed approach to plasma turbulence, very little work has been carried out specifically on ITG models. The reason is probably that ITG models require the solution of inhomogeneous SC's. Although codes that solve arbitrary SC's exist, numerical solutions of inhomogeneous SC's are rather computationally intensive [27]. As we have seen, most of the numerical effort has gone into direct simulations as described in Sec. 2.3. The topic of statistical closures for plasma turbulence is covered by another article in these Proceedings [28].

3 On the characteristic length and time scales of ITG turbulence

A primary goal in the current ITG research is the identification of the dependence of the characteristic length λ_c, time τ_c, and the average amplitude v_E of the turbulent velocity on whatever dimensionless control parameters occur in the model.

The conventional point of view is that ITG turbulence, as most types of electrostatic turbulence, is characterized by spatial scales much smaller than the size of the device. If this is the case, it is natural to expect that the transport observed across a region large compared to λ_c is diffusive, provided that the scale length of the temperature gradient is also large. One is tempted to assume that the local transport coefficient, defined as the ratio of the local heat flux to the temperature gradient, is a function of the control parameters through λ_c, τ_c, and v_E. For the turbulent ion heat conductivity one would have

$$\chi_i = (\lambda_c^2/\tau_c) f(v_E \tau_c/\lambda_c), \tag{11}$$

where $f(x)$ is some function.

An additional assumption, which is often implicitly made in dimensional estimates, is that v_E is of order λ_c/τ_c so that the function f is replaced by a constant. Thus the knowledge of λ_c and τ_c is usually deemed sufficient to estimate the transport.

One can see that this viewpoint calls for the validation of those otherwise unjustified assumptions. One can say that virtually all the most important open questions in plasma turbulent transport come from an examination of the validity of expressions like Eq. 11.

The question whether λ_c is much smaller than the machine size is the subject of this section. Even if this were the case, the expression 11 is per se questionable when it comes to evaluate the heat conductivity. Indeed, while one expects such a form to be valid for the diffusivity of tracers in a turbulent field, the temperature does not behave as the concentration of a tracer, but enters self-consistently in the dynamics of the velocity field. Thus there is no reason why the function f in Eq. 11

should depend only on $v_E \tau_c / \lambda_c$; one expects a general dependence on all the control parameters of the system. This hidden dependence would be even more important if coherent structures are present. In this case the assumption $v_E \sim \lambda_c / \tau_c$ could be grossly violated and the resulting difference would be substantial. This possibility and the role played by coherent structures will be discussed in Sec. 4.

More dramatic consequences on the evaluation of transport would occur if nonlocal effects are present. One obvious example of a nonlocal effect occurs when the total heat losses are controlled by some boundary layer. Although there is no compelling theoretical reason why it should be so, experiments seem to observe such effects in real systems in certain transport regimes. Thus it is useful to evaluate under what conditions such effects are expected (Sec. 5.1). When this occurs, the local profile must adjust to the given flux. Although the transport may be locally diffusive, the overall confinement is controlled by the boundary layer.

Finally, nondiffusive behavior is a theoretical possibility which one should not ignore (Sec. 5.2).

3.1 The correlation length of homogeneous turbulence

ITG is inherently an inhomogeneous turbulence problem. Inhomogeneity comes primarily from the radial dependence of the equilibrium magnetic field (magnetic shear) and from the poloidal dependence of the curvature operator. Implicit inhomogeneity also comes from the radial dependence of the temperature profile if the latter is allowed to vary.

Only in special conditions can the ITG model be treated as homogeneous. Since, however, most of our understanding of turbulence comes from the analysis of homogeneous problems, it is convenient to discuss what one may expect in general terms from plasma dynamics models.

In homogeneous situations the concept of cascade in wave-number space is particularly useful. The conventional approach is to assume that turbulence is injected locally in k-space (narrow-band injection) and propagates to regions where it is eventually dissipated by some damping mechanism. This approach, when applied to the ordinary Navier–Stokes fluids, has led to the classic concept of Kolmogorov cascade in three dimensions [29] and dual (energy and enstrophy) cascade in two dimensions [30].

In these idealized situations, the correlation length of homogeneous turbulence can usually be evaluated as the inverse of the low-k cutoff of the turbulent spectrum, the smallest wave-number band containing appreciable fluctuation energy. When the cascade occurs only towards small scales (as in 3D Navier–Stokes turbulence), this cutoff turns out to be of the same order as the energy injection wave-number band. In the presence of an inverse cascade, however, appreciable turbulent fluctuations would extend to lower wave numbers, until they are finally damped by some mechanism. Thus the low-k cutoff is determined by the balance between forcing and dissipation.

Little work has been done on the analysis of cascades in plasma dynamics models except for MHD and for the simple Hasegawa–Mima model [2, 31]. The reason is probably that energy injection in plasmas of interest is usually assumed to be broad band. Indeed, in the case of gradient-driven instabilities the growth-rate spectrum is rather wide, since it behaves typically as $\gamma(k) \sim k$ in the whole range between a low-k cutoff k_L, where it turns negative, and some high $k_{\text{peak}} \sim \rho_s^{-1}$ at which it peaks and then rolls over.

However, one should remark that the turbulent energy injection spectrum $\epsilon(k)$ can be estimated as the product $\epsilon(k) \sim \gamma(k)E(k)$ where $E(k)$ is the spectral energy density. Thus the real question is whether $\epsilon(k)$, which must be computed self-consistently, can be localized away from the dissipative cutoffs in order to have meaningful inertial ranges. In this instance it would be possible to evaluate the characteristic scales as well as the fluctuation energy without much trouble.

Thus the outcome would depend on the natural cascade dynamics of the model under consideration. For example, if the system "wants" to develop an inverse cascade spectrum such that $E(k) \sim k^{-\alpha}$ with $\alpha > 1$, as it is the case for the Hasegawa–Mima model [31], the resulting peak of $\epsilon(k)$ will quickly shift towards k_L. This would cause the relevant energy balance to take place in the same wave-number region, the energy-containing range. Although one could still take k_L as the inverse of the correlation length, it would be difficult to evaluate the fluctuation level in this conditions.

Such a shift of the peak of $E(k)$ from the peak of $\gamma(k)$ is commonly observed in numerical simulations and is also suggested from the experimental observations.

3.2 Mixing-length approach in fluid dynamics

Many phenomenological works in fluid dynamics are constructed around the mixing-length concept. In general, one deals with turbulence generated by some gradient of the average flow. The mixing length is introduced to relate the size of the fluctuations to the gradient of the flow.

Since ITG has strong formal similarity to turbulent convection, it is useful to review the mixing-length argument in the latter as an example.

Consider a fluid in the (constant) gravitational field subject to a temperature gradient. If the gradient points in the same direction as gravity, the fluid is unstable to convective motion. If the fluid is confined between two planes, the condition for instability is expressed in terms of the Rayleigh number

$$\mathrm{Ra} \equiv \frac{\Delta T \alpha_T g L^3}{\nu \chi} > \mathrm{Ra}_c, \tag{12}$$

where ΔT is the temperature difference across the system, L is the distance between the confining planes, α_T is the coefficient of thermal expansion, g is the gravitational acceleration, ν and χ are the (kinematic) viscosity and the thermal conductivity. The critical Rayleigh number Ra_c depend on the boundary conditions.

When the fluid is not confined (free turbulence), the condition 12 must be interpreted as determining the minimum unstable wavelength, where L is now a wavelength. We assume that condition 12 is well satisfied.

The mixing length l_c for this problem is introduced through the relation

$$\tilde{T} \approx l_c \nabla T. \tag{13}$$

The corresponding velocity fluctuation is estimated from the increment in kinetic energy when the fluid element moves a distance l_c in the buoyancy force:

$$\tilde{v} \approx (l_c \Delta T \alpha_T g)^{1/2} \approx l_c (\nabla T \alpha_T g)^{1/2}. \tag{14}$$

Thus one can estimate the heat flux as

$$\tilde{Q} \approx \tilde{v}\tilde{T} \approx l_c^2 (\nabla T)^{3/2} (\alpha_T g)^{1/2}. \tag{15}$$

So far these results depend on l_c, which is still undetermined. In general, one expects that l_c is a function of the average quantities and of the dimensionless parameters. Since one is effectively working at infinite Rayleigh and Reynolds number, one realizes that the only possibility is to take l_c to be of order of the temperature gradient scale-length:

$$l_c \sim L_T = T/\nabla T. \tag{16}$$

This gives

$$\tilde{T} \approx T \tag{17}$$

and

$$\tilde{Q} \approx T^2 (\nabla T)^{-1/2} (\alpha_T g)^{1/2}. \tag{18}$$

If we now assume that the heat flux is given, integration of Eq. 18 yields the one-third law [32] for the temperature profile:

$$T(z) \sim \left(\frac{Q^2}{\alpha_T g} \right)^{1/3} z^{-1/3}, \tag{19}$$

where z is a vertical coordinate along the direction of the gravity. [Note that $T(z)$ is actually the temperature difference between the observation point and infinity.]

Eq. 18 can also be obtained with a somewhat different physical argument. First we write the heat flux as a dimensional quantity times a function of the control parameters. It is customary to write

$$\tilde{Q} = \chi \nabla T f(\mathrm{Ra}, \mathrm{Pr}) \tag{20}$$

where $\mathrm{Pr} = \nu/\chi$ is the Prandtl number. Second, we postulate that, in the limit of $\nu \to 0$, $\chi \to 0$, and across a region $L = L_T$, the flux is independent of the dissipation coefficients. For this to be possible the function f must scale as

$$f(\mathrm{Ra}, \mathrm{Pr}) \sim (\mathrm{RaPr})^{1/2} \tag{21}$$

in that limit. One then recovers Eq. 18.

Thus one is tempted to conclude that the success of the mixing length approach is not casual. It stems from the lack of free parameters in the relevant limit. (See also Tennekes and Lumley [33] for a discussion on this point.) However, as already pointed out, even the simplest ITG model has enough free parameters that the estimate of the mixing length has a much greater degree of uncertainty.

3.3 Mixing length for ITG

For the ITG problem one can still assume a relation like Eq. 13. The problem is again to evaluate l_c.

Assume for the moment that one can entirely neglect the parallel dynamics. One is then left with Eqs. 1 and 3 with $v = 0$ and $\nabla_{\|} = 0$.

Consider also wave lengths such that $1 \ll k_\theta \ll \rho_*^{-1}$, so that they are sufficiently long that the finite Larmor radius corrections are negligible but sufficiently short that the curvature can be considered constant (local approximation). It is also convenient to separate the average temperature from the fluctuating part: $T = T_o + \tilde{T}$. In this situation, the control parameters can be absorbed in the normalization by a rescaling to new length and time units L_T and $L_T^2/[D_B(2L_T/R)^{1/2}]$:

$$\partial\phi/\partial t + \partial_y \tilde{T} = 0. \tag{22}$$

$$d\tilde{T}/dt + \partial_y \phi = 0, \tag{23}$$

where ∂_y is the derivative in the poloidal direction. (Note that ϕ has been left out from Eq. 22 since the rescaling $\phi \to (2L_T/R)^{1/2}\phi$ makes apparent that ϕ is subdominant with respect to $\tilde{T}$ in that equation.) No explicit parametric dependence is left in this modified ITG model. The situation is similar to turbulent convection, as previously discussed. Indeed, the analogy is even closer when one considers that Eqs. 22–23 are homologous to the two-dimensional Boussinesq system, where ϕ is replaced by $\nabla^2\phi$

in the first term of Eq. 22. The heat flux is then obtained from dimensional analysis:

$$\tilde{Q} \sim \frac{cT_e}{eB}(2L_T/R)^{1/2}T_e/L_T. \tag{24}$$

This monstrous value (corresponding to a thermal conductivity essentially at the Bohm level cT_e/eB) is easily understood from the analysis of the previous section. It corresponds to the assumption that the mixing length is of order of the temperature gradient length which is typically of order a. Then use of Eq. 11 with $\phi \approx T_e/e$ gives an estimate comparable to Eq. 24.

This value exceeds the experimental observation by three or four orders of magnitude. Thus one should assume that the mixing length is much smaller than so far estimated.

The origin of the discrepancy can be traced to the neglect of the parallel dynamics. Note that this is equivalent to treating the auxiliary parameter A of Eqs. 1–3 as independent and setting it to zero. However, $A \gg 1$ in the situations of interest. In this case the sound waves propagating along the field lines strongly limit the radial and poloidal size of the fluctuations. This can be seen from the linear theory treatment, where the parallel derivative operator is replaced by an effective $k_\parallel$ and taken to be constant: $\nabla_\parallel \to ik_\parallel^{\text{eff}} \approx i/(qR)$. The longest poloidal wavelength of an unstable mode is obtained from the condition 8:

$$\omega_{*T} \approx k_\parallel^{\text{eff}} c_s. \tag{25}$$

This gives the estimate

$$k_\theta \approx L_T/(qR\rho_s). \tag{26}$$

One then invokes two more assumptions about the turbulent dynamics. First one assumes, as discussed in Sec. 3.1, that some kind of inverse energy cascade is at work. The result would be an accumulation of energy in the region of the long-wave-length cutoff as given by Eq. 26. The second assumption, which is suggested by the results of most of the direct simulations, is that the turbulence spectrum is essentially isotropic. Therefore one is tempted to conclude that

$$l_c \approx 1/k_\theta \approx qR\rho_s/L_T. \tag{27}$$

One can see from this expression that the mixing length is now proportional to the small scale ρ_s. One expects much lower transport than 24. However, even assuming 27, there is some degree of uncertainty in the choice of the time scale.

For the situations of interest one usually assumes that the strongest drive is the coupling between the temperature gradient and the curvature operator. One then balances the time derivative of ϕ with the curvature term in Eq. 1. Upon using also Eq. 13, one ends up with the estimates

$$\tau_c^{-1} \approx (\epsilon \nabla T)^{1/2} k_\theta \tag{28}$$

and, upon restoring the dimensions,

$$\chi \approx \frac{cT_e}{eB} \frac{R^{1/2}}{L_T^{3/2}} q \rho_s. \tag{29}$$

However there are other possibilities. One can balance the time derivative with other terms, thus obtaining a different result. One can also estimate the inverse time as the maximum growth rate, which would give $\tau_c^{-1} \approx (\epsilon \nabla T)^{1/2}$ instead of Eq. 29. The result would be somewhat different [34]:

$$\chi \approx \frac{cT_e}{eB} \frac{R^{3/2}}{L_T^{5/2}} q^2 \rho_s. \tag{30}$$

One could debate the merits of one choice rather than the other or of any other possible expression, by looking, for example, at the experimental results. However this may not be too relevant because ITG is an approximate model. It would also not be satisfactory from the theoretical point of view.

Thus one is still left with big uncertainties in the evaluation of the mixing length. The only common parametric dependence in the above estimates is that l_c scales with ρ_s.

As previously discussed in Sec. 2.2, even this conclusion is objected to by some researchers on the grounds that linear theory in toroidal geometry produces eigenfunctions whose radial extension scales as $(\rho_s a)^{1/2}$. It is then argued that this scale should be used an estimate of λ_c.

One should note, however, that extended radial eigenfunctions are not unique to toroidal geometry. In a shearless slab, for example, the radial extension of the fastest growing mode is of order of the slab width. Such structures often break up in the nonlinear regime, as observed, with few exceptions [35], in several numerical simulations; see for example [36].

A mechanism for the breakup of elongated radial structures due to secondary instabilities has been proposed and analyzed by Cowley *et al.* [12]. Elongated (say, elliptical) structures experience strong gradients in the direction of their minor axis. This gradients are the drive of the secondary instability through a mechanism analogous to the primary ITG instability. Qualitatively, the resulting structures must be roundish in order to be robust to the secondary instabilities. This explains the isotropization of the spectrum observed in many simulations, but does not give information about the size of the structures and hence of the coherence length of turbulent fluctuations.

Although this issue is still open, it seems natural to argue that the linear radial structure, which is brought in by the weak toroidal coupling between cylindrical eigenfunctions, should not survive the stronger interactions experienced in the nonlinearly saturated state.

Besides the results of local simulations, the breakup of the linear structures is clearly documented in the recent global toroidal particle simulations of Mynick and Parker [37] and of the Horton–Tajima group [38]. These simulations indicate that the saturated state contains radially extended structures with a machine size dependence in the radial correlation length. As an example, Fig. 1 shows the evolution of the system from a state with extended toroidal eigenmodes [frame (a)] to the partially circularized structures of frames (b) and (c).

Both papers report a scaling $\lambda_c \sim \rho_s^{1-\alpha} L_T^{\alpha}$ with the exponent in the range $0.3 < \alpha < 0.5$. Thus although the linear structures do break up, some dependence on the macroscopic scale seems to be retained even in the nonlinear regime. The temperature profile relaxes toward a marginally stable state with $L_T \approx L_{T\mathrm{crit}}$, which may partially account for the preservation of the extended structures. One should also remark that these simulations were performed at $\rho_* \approx 10^{-2}$. This may also be a source of discrepancy with the local simulations which are performed at $\rho_* \approx 10^{-3}$, if a transition in the scaling occurs at some intermediate ρ_* as suggested by Hammett [39].

Clearly the above discussion shows that the question of the λ_c scaling is still wide open and that it is probably the most urgent issue to address in future investigations.

3.4 Quasilinear estimates

A large body of literature has been devoted to the computation of transport coefficients with quasilinear theory (QLT). In QLT fluctuations are treated linearly. Thus the information about the fluctuation level is not derived internally in the theory; one must rely on some independent estimate. This is normally done with a mixing-length relation like Eq. 16. This in turn depends on the assumption made on l_c. Thus one sees that, besides the obvious criticism that phase relations between the fields are not taken into account properly [40] (more will be said in this respect in Sec. 4), one can easily conclude that, despite the detailed calculations, QLT is in essence not better than the simpler mixing-length analysis previously outlined.

4 Coherent Structures

In both neutral fluids and plasmas, turbulence often manifests itself in a dual fashion. One aspect is the occurrence of broadband, space-filling fluctuations (waves or modes) which in certain conditions are organized in a self-similar, Kolmogorov-like spectrum. The other aspect is the formation of long-lived nonlinear coherent structures (CS) (vortices or solitons) embedded in a background of weaker fluctuations.

With the exception of systems exhibiting marked solitonic behavior, the treatment of turbulence as interacting waves has been the prevailing one, possibly because of the large amount of work on homogeneous turbulence and the interest in spectral cascades, which makes the use of Fourier amplitudes a natural choice for the fundamental variables.

Only in the last decade or so has there been a revived interest in describing turbulent phenomena in real space. This is in part due to the increased use of powerful numerical simulations that have allowed scientists to study the various processes occurring during the evolution of systems of many interacting vortices, like vortex generation and mergers. One of the best known results is the discovery of the formation of long-lived vortices in two-dimensional Navier–Stokes simulations [41]. This, together with the observation that 2D NS does not exhibit Kraichnan's[30] k^{-3} law in the enstrophy cascade range [41, 42, 43] has prompted a debate on the role of vortices in spectral cascades.

Isolated coherent structures (particularly the dipolar vortex or modon) have been employed to describe certain phenomena in atmospheric dynamics [44]. In plasmas, the conditions for the existence of coherent structures have been analyzed in various drift-wave models [45, 46].

Energetically, the coherent structures arise through self-organization as an efficient way for the plasma to store free energy and momentum. The mechanism for the creation of the coherent structures is through the coalescence and merging of aligned patches of vorticity (angular momentum). Both neutral-fluid simulations and plasma simulations see the tendency in the long-time limit for the turbulence to relax to states with large-scale coherent structures, predominantely in the form of monopolar and dipolar vortices. Other factors, however, can mitigate against the formation of CS including strong, broadband spectral regions of growth or damping and sufficiently strong spatial inhomogeneities such as a strongly sheared magnetic field or sheared mass flow.

The variety of conditions and types of CS implies that it is difficult to give a general and at the same time quantitatively satisfactory definition. It is useful to employ the following qualitative definition [47], reserving more detailed definitions for specific applications.

Coherent structures are localized structures containing significant energy and momentum, with a resiliency to external perturbations so that their *lifetime is long compared to the wave dispersion time for a linear structure of the same scale.*

Often CS are characterized by the approximate fulfillment of some kind of functional relation between interacting fields (dynamic alignment). The usual consequence is that the nonlinearity describing the interaction between those fields can almost vanish in the region occupied by the CS. In the 2D Navier–Stokes equation this occurs between the stream function ψ and the vorticity $\nabla^2\psi$:

$$\left[\psi, \nabla^2\psi\right] \approx 0. \tag{31}$$

Coherent structures in the 3D Navier–Stokes equation show alignment between the velocity and the vorticity (Beltramization). In plasmas, relations like Eq. 31 are used in the explicit construction of CS [45, 46]. The force-free states that result from Taylor's relaxation [48] in 3D magnetohydrodynamics can be viewed as CS.

Another feature of CS is that when they are present at a substantial density, certain fields show a high degree of spatio-temporal intermittency and non-Gaussian statistics. The paradigm for this is again the 2D NS equation. The vorticity tends to concentrate in the regions where Eq. 31 is satisfied. The resulting probability density function exhibits non-Gaussian tails with high kurtosis. We refer the reader to Ref. [28] for an extended discussion of intermittent statistics with some applications to plasmas.

We now specifically consider how coherent structures can affect the overall transport in plasma models like ITG.

We first consider how the presence of long-lived structures can affect the estimate of the transport coefficients. Going back to Eq. 11, one can sensibly take the average CS lifetime as a measure of the (Eulerian) correlation time τ_c, whereas λ_c can be taken as the typical size of the CS. For long-lived structures τ_c must be longer than the typical turnaround time λ_c/v_E. Thus one is interested in the behavior of Eq. 11 when the $\mathbf{E} \times \mathbf{B}$ rotation number R_E (also called Kubo number in the context of passive advection [49]) is large:

$$R_E \equiv v_E \tau_c / \lambda_c > 1. \tag{32}$$

The classical treatment of the large-rotation-number regime predicts a linear behavior for the function appearing in Eq. 11, $f(R_E) \sim R_E$. This gives

$$\chi \sim v_E \lambda_c \qquad (R_E \gg 1). \tag{33}$$

The latter estimate is challenged by a detailed analysis of the particle dynamics in 2D flows with high Kubo number K [50]. This work predicts the scaling $f(K) \sim K^{7/10}$. Good agreement with the qualitative features of Ref [50] has been found by numerical simulations at extremely high $K \sim 10^4$, although there is some disagreement in the resulting exponent [51, 52]. Note that, experimentally, the Kubo number of $\mathbf{E} \times \mathbf{B}$ turbulence does seem to fall in the range 1 to 10. So, for any practical purpose one can use Eq. 33 as an upper bound.

More dramatic consequences can occur because of the dynamic alignment. When this occurs between the advecting field and some advected scalar, there is a substantial reduction in the transport of that scalar. In ITG turbulence, the relevant condition is a functional relation between temperature and electric potential:

$$[\phi, T] \approx 0. \tag{34}$$

In the region where this occurs $T = T(\phi)$ and the contribution to the heat flux from that region vanishes:

$$\int_{\mathrm{CS}} \mathbf{v}_E T dV = 0, \tag{35}$$

where the integral is over a closed region bounded by an isoline of ϕ.

A result in this sense was found for the 2D shearless ITG model numerically investigated in Ref. [36]. In this work it was found that the heat flux can be substantially lower than expected from conventional (quasilinear) estimates. At the same time, large regions of the computational domain where Eq. 34 is approximately valid were observed. Also a change in the parametric dependence of transport on the control parameters was reported, with the resulting heat flux depending explicitly on the dissipation coefficients. Qualitatively, this is not too surprising in the light of the previous discussion. Since the contribution of the CS to transport tends to vanish, the remaining parametric dependence must come from the boundary region between the CS. In these regions the dissipation is effective, due to the presence of sharp gradients. A reduction in the transport was also observed in 2D (single helicity) ITG simulation with shear [53], although in this case the role of CS is less evident.

What is missing here is a quantitative theory that links the correlation function of T and ϕ to the control parameters and in particular the Reynolds-like numbers. In any case the above results cast doubts on the utility of Eq. 11 when strong CS are present. Although one may still be able to describe the transport as a diffusion process, it seems unlikely that one can find a universal parametrization of the transport coefficients in terms of the three quantities v_E, τ_c and λ_c.

It remains to be seen whether CS play an important role in the more general 3D ITG model we are discussing in this work. One can certainly construct three-dimensional ITG coherent structures [45, 46], but the key questions are whether they evolve spontaneously from the background of wavelike ITG fluctuations and whether they affect significantly the ensuing transport. Good candidates for 3D ITG CS are the objects shown in Fig. 1, as discussed in Sec. 3.3.

5 Nonlocal Effects

In this section we consider for completeness two types of nonlocal effects that may play a role in the global transport scaling of a plasma system. In the next subsection we discuss how a thermal boundary layer can control the overall heat losses in convective turbulence. In the other subsection we consider what might happen if the diffusion approximation breaks down.

It is worth remarking that the main motivation behind the following pages comes from the experimental debate. It is often reported that confinement devices exhibit a variety of nonlocal effects, such as transport barriers at the plasma boundary (or even in its interior) and global, abrupt changes of the transport coefficients. The interpretation of the propagation of perturbations, whether artificially induced or following spontaneous relaxation events, is also considered problematic.

It is therefore natural to explore to what extent a paradigm model like the one discussed in this work could reproduce those features.

5.1 Boundary effects

We consider now the effect of the boundary conditions on the overall transport scaling laws. To this end it is again useful to review the Rayleigh Benard problem as a guide to what one may expect in more complicated situations. Therefore, let us consider the effect of a rigid wall perpendicular to the direction of the heat flux.

Since the velocity perpendicular to the wall vanishes at the boundary, so does the turbulent heat flux. Thus near the wall the heat must be carried by collisional thermal conduction. This leads to the formation of a thermal boundary layer whose width is determined by the condition that the layer is stable to the onset of convection ($\mathrm{Ra} \approx \mathrm{Ra}_c$). For a given heat flux Q one has

$$\frac{\Delta T_{\mathrm{BL}} \alpha_T g \delta_{\mathrm{BL}}^3}{\nu \chi} \approx \mathrm{Ra}_c, \tag{36}$$

$$\chi \frac{\Delta T_{\mathrm{BL}}}{\delta_{\mathrm{BL}}} \approx Q. \tag{37}$$

This gives an estimate for the boundary layer width δ_{BL} and temperature jump ΔT_{BL}

$$\delta_{\mathrm{BL}} \approx \left(\frac{Ra_c \nu \chi^2}{\alpha_T g Q} \right)^{1/4}. \tag{38}$$

$$\Delta T_{\mathrm{BL}} \approx \left(\frac{Ra_c \nu Q^3}{\alpha_T g \chi^2} \right)^{1/4}. \tag{39}$$

At a distance from the wall greater than δ_{BL} the usual free-turbulence estimate of Eq. 19 applies. The temperature jump across the free-turbulence region can be estimated by setting $z \approx \delta_{\mathrm{BL}}$ in Eq. 19. Upon ignoring numerical factors and the dependence on the Prandtl number, one obtains again Eq. 39. Still, because of the power-law dependence of Eq. 19, most of the contribution comes from the region around the boundary layer.

Thus one can reach the surprising conclusion that although most of the system can be possibly described by the free-turbulence treatment of Sec. 3.2, the actual temperature jump across the whole system is mainly determined by the presence of the thermal boundary layer.

This result is usually seen in the context of the problem of convection between plates, when the fluid is confined between two walls. In this case the temperature difference is usually taken as the control variable, while the flux is determined or measured. By solving Eq. 39 for the flux and taking $T_{BL} \approx \Delta T$ one recovers the known result:

$$Q \sim \frac{\chi \Delta T}{L} \left(\frac{Ra}{Ra_c} \right)^{1/3} . \qquad (40)$$

This expression, which has been confirmed experimentally at moderate Rayleigh numbers [54], differs from the scaling one would obtain by ignoring the boundary layer, which is obtained by taking $z \sim L$ in Eq. 19.

The above discussion and the similarity of ITG with thermal convection prompts the natural question whether boundary layer effects are important also for plasma transport. This in turn leads to the question of what are the appropriate boundary conditions for the ITG model.

A boundary condition that is simple to implement is the rigid wall of the previous example, when the radial velocity at the boundary is set to zero. This type of boundary condition has been often used in numerical simulations. Naturally, the formation of thermal boundary layers is expected in this case and has often been reported.

However, it is not clear whether this type of boundary layer has anything to do with reality. The point is that confined plasmas are not directly in contact with the walls; rather, they communicate with the outer world via a region of cold plasma, the so-called scrape-off layer (SOL) that lies between the well confined plasma and the machine walls. In the SOL, the magnetic field lines are open and connect material components of the device. Thus the actual boundary conditions one would ideally like to implement are flux conditions at the end of the field lines in the SOL.

At the main plasma–SOL interface (the outermost region where the ITG model can be of some utility) substantial turbulence is expected (and observed). Thus the turbulent transport cannot be neglected there. At the same time the plasma becomes cooler and the collisional transport can become important (as in the usual boundary layers). Direct (ballistic) losses of particles and energy into the SOL also occur.

One should also say that a variety of experiments suggest that large modifications of the plasma parameters at the plasma boundary occur when changes in the confinement regimes take place. More generally, correlations between the boundary parameters (like the ion temperature) and the confinement indicators are sometimes reported. This is reminiscent of the thermal convection problem where the boundary temperature correlates with the stored energy of the system.

This suggests that some kind of boundary-layer phenomena may be at work. Whether the ITG model, with some proper choice of the boundary conditions, is suitable for the investigations of this phenomena is an open question.

5.2 Nondiffusive effects

Nondiffusive transport occurs in many systems as a consequence of long-range correlations. For example, diffusive transport of tracers in fluids is guaranteed by the central limit theorem (CLT) [55] if the time scale over which the transport process is observed is sufficiently long (usually longer than the Eulerian correlation time) that consecutive particle displacements are only weakly correlated. Thus nondiffusive behavior occurs when the conditions for the validity of the CLT are not satisfied (see Ref. [56] for an extended discussion).

In turbulent systems this can occur in the spectral ranges below the correlation length. An example is the Richardson's law of particle displacement in the Kolmogorov spectrum. In principle, nondiffusive behavior can also occur at scales above the correlation length. Thus transport of tracers in two-dimensional turbulence can be nondiffusive in some intermediate range [51] $\lambda_c \ll l \ll \lambda_M$, where λ_M is the Lagrangian correlation length, although this requires that the Kubo number is much higher than usually observed in laboratory plasmas.

As we have seen, theoretical considerations as well as experimental evidence seem to rule out the possibility that the correlation length is comparable to the macroscopic length a. Thus one expects that there is a range in scales at which transport is diffusive. In particular, this would suggest that global transport can be modeled with diffusion equations.

Things can be different for perturbative transport. Clearly, if a perturbation has initially characteristic scales that are substantially shorter than λ_c, the perturbation will initially evolve with nondiffusive dynamics. This might explain some of the conflicting experimental observations.

One must also remember that the test-particle approach for the estimate of the transport coefficient treats the correlations between the fields incorrectly. This can lead to a poor evaluation of the transport coefficient, as discussed in Sec. 4. It can even generate paradoxes, like the one occurring in this ITG model, as well as in any other model with adiabatic electron response. One could naively estimate the particle diffusivity from the knowledge of the fluctuating potential. This would be wrong (and appropriate only for real impurities), since the adiabaticity constraint forces the density transport to zero, independently of the features of the ambient turbulence.

It seems that one should leave open the possibility that, although turbulence is small scale, the heat flux at a point may not be parametrizable as a unique function of the local average fields and their first derivatives.

This poses a methodological problem. The usual approach to turbulent transport (see Sec. 2.3) is to assume a given gradient and to derive the local transport coefficients as a local function of that gradient. However, this will give an ambiguous result if the dependence of the flux on the profiles is a more general function(al).

The natural way to avoid this uncertainty is to consider the inverse problem, which means to prescribe the amount of heat carried out of the system and to derive the *total* temperature (fluctuating *and* average). This choice is in line with real experiments where the input power is a control parameter. It can be easily implemented in global simulations and, with some difficulty, as a flux boundary condition at the inner boundary in local simulations [57]. It is important to stress that the resulting temperature profile is the "natural" one for the problem at hand.

Future studies on the ITG model with flux boundary conditions have the potential to settle the local/nonlocal transport controversy. Clearly, one must also allow the possibility that these effects are present in the experiment, but that the ITG model that has been the subject of this paper is missing some crucial ingredient.

6 Conclusions

In this work a simple ITG model has been introduced as an instrument to discuss a number of key questions in plasma turbulence theory. We have especially emphasized the issues connected with the problem of turbulent transport in magnetically confined plasmas. This model contains the basic ingredients of more general models, such as the gradient drive, the magnetic shear and curvature, and the ion Landau damping, without unwanted complications. It may turn out to be a useful paradigm for turbulent transport in toroidal plasmas.

Virtually all the open problems discussed hinge around the use and validity of the local, diffusive approximation and its parametrization in terms of the control parameters of the model.

Perhaps the most urgent problem is to determine the parametric dependence of the correlation length, time, and fluctuation magnitude of the ITG model. As we have seen, it may turn out to be particularly crucial to assess the dependence on the scale separation parameter ρ_*. On the one hand, this will contribute to our understanding of some of the mechanisms at work in ITG turbulence. On the other hand, it could provide a practical contribution to the debate of how to extrapolate the information of the existing transport databases to future devices.

Understanding what role the coherent structures could play in the transport scaling of ITG turbulence is also a major area of future research. The characterization of these objects, which are nontrivially three-dimensional, will require the development of special diagnostics of the output of the simulations.

Finally, the possibility that nonlocal effects are important should not be underestimated. Our discussion was prompted by the experimental debate and by the general awareness of their importance in fluid dynamics, although the present theoretical understanding of these issues in the case of plasmas is rather modest. Two kinds of nonlocal effects have been considered. In the first, boundary layers may dominate the overall transport by acting as barriers. The bulk of the system would still be described in terms of diffusive transport but the global scaling is determined by the boundary-layer scaling. The second type of nonlocal effect is substantially deeper and involves the very notion of diffusive transport.

Naturally, substantial progress in this field would come from the interplay between carefully designed numerical simulations of paradigm models and a general conceptual understanding of the turbulence mechanisms.

Acknowledgments

The authors enjoyed many stimulating discussions with the partecipants in the 1995 ITP Workshop on Turbulence and Intermittency in Plasmas.

This work was supported in part by the National Science Foundation Grant No. PHY94–07194 and in part by U.S. Dept of Energy Contracts DE–FG05–80ET–53088 and DE–AC02–76–CHO–3073. M. A. Beer was supported in part by an appointment to the U.S. Department of Energy Fusion Energy Postdoctoral Research Program administered by the Oak Ridge Institute for Science and Education.

References

[1] M. C. Zarnstorff, S. Batha, A. Janos, F. L. Levinton, and the TFTR Group, in Local Transport Studies in Fusion Plasmas, J. D. Callen, G. Gorini, E. Sindoni, Eds., Societa Italiana di Fisica, Bologna (1993).

[2] A. Hasegawa and K Mima, Phys. Rev. Lett. **39**, 205 (1977).

[3] P. Terry and W. Horton, Phys. Fluids **25**, 491 (1982).

[4] S. I. Braginskij, in *Reviews of Plasma Physics*, edited by M. A. Leontovich, Consultants Bureau, New York (1985), Vol. 1, p. 285.

[5] G. W. Hammett and F. W. Perkins, Phys. Rev. Lett. **64**, 3019 (1990).

[6] G. W. Hammett, W. Dorland and F. W. Perkins, Phys. Fluids **B4**, 2052 (1992).

[7] W. Dorland and G. W. Hammett, Phys. Fluids **B5**, 812 (1993).

[8] G. W. Hammett, M. A. Beer, W. Dorland, S. C. Cowley and S. A. Smith, Plasma Phys. and Contr. Fusion **35**, 973 (1993).

[9] W. Dorland, *Gyrofluid Models of Plasma Turbulence*, Ph.D. thesis, Princeton University (1993).

[10] M. A. Beer, *Gyrofluid Models of Turbulent Transport in Tokamaks*, Ph.D. thesis, Princeton University (1995).

[11] J. W. Connor, R. J. Hastie and J. B. Taylor, Proc. R. Soc. London A **365**, 1 (1979).

[12] S. C. Cowley, R. M. Kulsrud and R. Sudan, Phys. Fluids **B3**, 1803 (1991).

[13] W. Horton, D.-I. Choi and W. M. Tang, Phys. Fluids **24**, 1077 (1981).

[14] F. Romanelli, Phys. Fluids **B1**, 1018 (1989).

[15] L. Chen, S. Briguglio and F. Romanelli, Phys. Fluids **B3**, 611 (1991).

[16] J. W. Connor, J. B. Taylor and H. R. Wilson, Phys. Rev. Lett. **70**, 1063 (1993).

[17] F. Romanelli and F. Zonca, Phys. Fluids **B5**, 4081 (1993)

[18] J. Y. Kim and M. Wakatani, Phys. Rev. Lett. **73**, 2200 (1994).

[19] R. E. Waltz, G. D. Kerbel and J. Milovich, Phys. Plasmas **1** 2229 (1994).

[20] W. Horton, R. D. Estes and D. Biskamp, Plasma Physics **22**, 663 (1980).

[21] M. A. Beer, S. C. Cowley, and G. W. Hammett, Phys. Plasmas **2**, 2687 (1995).

[22] S. E. Parker and W. W. Lee, Phys. Fluids **B5**, 77 (1992), and references therein.

[23] S. E. Parker, W. W. Lee, and R. A. Santoro, Phys. Rev. Lett. **71**, 2042 (1993).

[24] R. J. Fonck, G. Cosby, R. D. Durst, S. F. Paul, N. Bretz, S. Scott, E. Synakowski, and G. Taylor, Phys. Rev. Lett. **70**, 3736 (1993).

[25] E. A. Frieman and L. Chen, Phys. Fluids **25**, 502 (1982).

[26] M. Kotschenreuther, W. Dorland, M. A. Beer, and G. W. Hammett, Phys. Plasmas **2**, 2381 (1995).

[27] J. A. Krommes, *Topics in the theory of statistical closure approximations for plasma physics*, in "Statistical Physics and Chaos in Fusion Plasmas", p. 241, C. W. Horton and L. E. Reichl Eds., Wiley, New York (1984).

[28] J. A. Krommes, *Systematic statistical theories of plasma turbulence and intermittency: Current status and future prospects*, these proceedings.

[29] A. N. Kolmogorov, C. R. Acad. Sci. U.S.S.R. **30** 301 (1941).

[30] R. Kraichnan, Phys. Fluids **10**, 1417 (1967).

[31] M. Ottaviani and J. A. Krommes, Phys. Rev. Lett. **69**, 2923 (1992).

[32] A. S. Monin and A. M. Yaglom, *Statistical Fluid Mechanics*, MIT Press, Cambridge, MA (1971).

[33] H. Tennekes and J. L. Lumley, *A First Course in Turbulence*, MIT Press, Cambridge, MA (1972), p. 57.

[34] M. Ottaviani, W. Horton and M. Erba, *Thermal transport from a phenomenological description of ion-temperature-gradient-driven turbulence*, in preparation (1995).

[35] J. F. Drake, P. N. Guzdar and A. Dimits, Phys. Fluids **B3** 1937 (1991).

[36] M. Ottaviani, F. Romanelli, R. Benzi, M. Briscolini and S. Succi, Phys. Fluids **B2**, 67 (1990).

[37] H. E. Mynick and S. E. Parker, Phys. Plasmas **2**, 2231 (1995).

[38] Y. Kishimoto, T. Tashima, W. Horton, M. J. Le Brun and J. Y. Kim, IFS report n. 711 (1995), to appear in Phys. of Plasmas.

[39] G. W. Hammett et al., Proc. of the 15-th International Conference on Plasma Physics and Contr. Nucl. Fusion Research, paper IAEA-CN-60/D-2-II-1, IAEA (1994).

[40] G. Hu, J. A. Krommes and J. C. Bowman, Phys. Lett. A **202**, 117 (1994).

[41] J. C. McWilliams, J. Fluid Mech. **146**, 21 (1984).

[42] A. Babiano, C. Basdevant, B. Legras and R. Sadourny, J. Fluid Mech. **183**, 379 (1987).

[43] P. Santangelo, R. Benzi and B. Legras, Phys. Fluids **A1**, 1027 (1989).

[44] V. D. Larichev and G. M. Reznik, Dokl. Akad. Nauk. SSSR **231**, 1077 (1976).

[45] W. Horton, Phys. of Fluids **B1**, 524 (1989).

[46] W. Horton, J. Liu, J. D. Meiss and J. E. Sedlak, Phys. of Fluids **29**, 1004 (1986).

[47] W. Horton and S. Benkadda, Proc. of the 1995 workshop on "Transport, Chaos and Plasma Physics", Marseille (1995).

[48] J. B. Taylor, Phys. Rev. Lett. **33**, 1139 (1974).

[49] J. A. Krommes. Statistical descriptions and plasma physics. In *Handbook of Plasma Physics*, vol. 2, A. A. Galeev and R. N. Sudan Eds., North Holland, Amsterdam (1984).

[50] A. V. Gruzinov, M. B. Isichenko and Ya. L. Kalda, Sov. Phys. JETP **70**, 263 (1990).

[51] M. Ottaviani, Europhysics Letters **20** 111 (1992).

[52] M. B. Isichenko, W. Horton, D. E. Kim, E. G. Heo and D.-I. Choi, Phys. of Fluids **B4**, 3973 (1992).

[53] B. G. Hong and W. Horton, Phys. of Fluids **B2**, 978 (1990).

[54] B. Castaing, G. Gunaratnae, F. Heslot, L. Kadanoff, A. Libchaber, S. Thomae, X.-Z. Wu, S. Zaleski and G. Zanetti, J. Fluid Mech. **204**, 1 (1989).

[55] B. V. Gnedenko and A. N. Kolmogorov, *Limit Distributions for Sums of Independent Random Variables*, Addison-Wesley, Reading, MA (1954).

[56] J. P. Bouchod and A. Georges, Phys. Rep. **195**, 127 (1990).

[57] B. D. Scott, Proc. of the 22-nd European Physical Society Conf. on Contr. Fusion and Plasma Physics, Bournemouth (1995), vol. 19C, part I, p. 229.

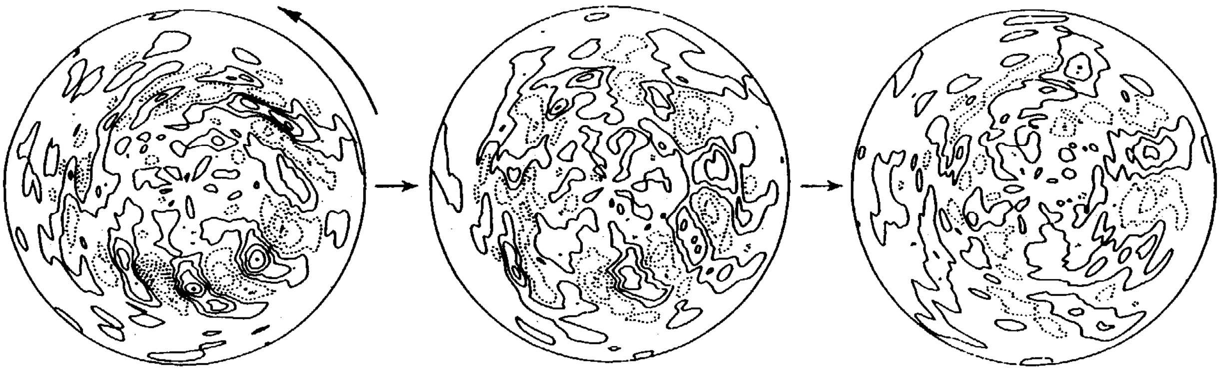

(a) $t=3500\ \omega_{ci}^{-1}$ (b) $t=5600\ \omega_{ci}^{-1}$ (c) $t=11400\ \omega_{ci}^{-1}$

Fig. 1. Poloidal cross section showing the isolines of ϕ from the full torus particle simulations of Ref. [38]. (a) linear phase; (b) during saturation; (c) at saturation.